공학석사 학위논문

A study on influences of interfacial progressive-partial debonding on fracture toughness enhancement of polymer nanocomposites: multiscale finite element analysis

계면 진전 부분 분리에 따른 폴리머 나노복합재의 인성 향상에 대한 멀티스케일 유한 요소 해석

2018 년 2 월

서울대학교 대학원

기계항공공학부

한진규

A study on influences of interfacial progressive-partial debonding on fracture toughness enhancement of polymer nanocomposites: multiscale finite element analysis

계면 진전 부분 분리에 따른 폴리머 나노복합재의 인성 향상에 대한 멀티스케일 유한 요소 해석

지도교수 조 맹 효

이 논문을 공학석사 학위논문으로 제출함

2018 년 1 월

서울대학교 대학원

기계항공공학부

한 진 규

한진규의 공학석사 학위논문을 인준함

2018 년 1 월

위 원 장 _____ **(인)**

부위원장 _____ **(인)**

위 원 _____ **(인)**

Abstract

A multiscale analysis is performed to observe fracture toughness enhancement of the epoxy-silica nanocomposites when interfacial progressive-partial debonding of nanoparticles occurs. Allegedly, interfacial debonding-induced nanovoid growth is one of the main toughening mechanisms and it consists of two sub-mechanisms – interfacial debonding of nanoparticles and subsequent plastic yielding of matrix. Multiscale framework of both toughening sub-mechanisms considering interfacial progressive-partial debonding (IPPD) of nanoparticles is constructed. To investigate the effects of the toughening mechanisms by confirming the microscopic stress fields of the nanocomposites, finite element (FE) models that include progressive-partial debonding of interfacial area are constructed. An influence of the area with IPPD on the dissipated plastic energy of matrix domain is investigated. This paper provide insights for applying the IPPD phenomenon in analysis on the toughness enhancement of nanocomposites by considering the results of the multiscale analysis model.

Keywords : Nanocomposites, Energy dissipation, Toughening mechanism, Interfacial progressive-partial debonding, Multiscale analysis

Student ID : 2014-22475

Table of Contents

List of tables

List of figures

1. Introduction

The crosslinked epoxy-based material systems are widely used due to their high modulus and low coefficient of thermal expansion [1-3]. However, the formation of highly crosslinked network causes high brittleness of epoxy-based material systems, which results in low fracture toughness. Actually, the fracture toughness of materials is critically dependent on the critical strain energy release rate, which is the summation of surface energy and plastic deformation energy. Allegedly, the fracture toughness of polymer nanocomposites is enhanced especially when the silica nanoparticles [4-14] are added into the epoxy domain. Reportedly, the embedded nanoparticles enhanced the fracture toughness of polymer nanocomposites by promoting toughening mechanisms including the interfacial debonding-induced nanovoid growth and localized shear banding mechanisms [8, 15-19, 28]. These toughening mechanisms cause dissipation of the surface energy and plastic deformation energy, which results in improvements of fracture toughness of polymer nanocomposites. Between the aforementioned two main toughening mechanisms, I focused on the interfacial debonding-induced nanovoid growth mechanism. An experimental observation of the mechanism is represented in Figure 1 (a) and (b).

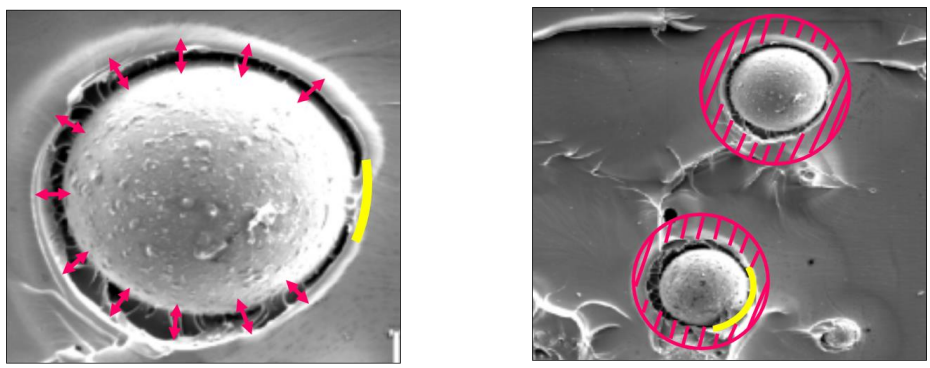

(a) (b)

Figure 1. Experimental observation of the interfacial debonding-induced nanovoid growth toughening mechanism [16] with surface contact described in yellow curve: (a) interfacial debonding between particle and matrix and (b) plastic yielding of matrix described in red striped zone around the particles.

For the interfacial debonding-induced nanovoid growth mechanism, Zappalorto M *et al*. [17-19] proposed an analytic form of multiscale model to predict fracture toughness enhancement of polymer nanocomposites. This multiscale model is based on the assumption that the nanoparticles are uniformly debonded from the matrix without any processual partial contact when the nanoparticles are subjected to the critical value of stress. However, in actual case, interfacial debonding of nanoparticles undergoes progressive debonding sequence of which an intermediate snapshot is described in the lower nanoparticle of Figure 1 (b). In spite of the merit on the simple description of representative volume element (RVE), the proposed analytic model has limitation on the description of the interfacial progressive-partial debonding (IPPD) of nanoparticles.

There have been several studies on the interfacial partial debonding of elastoplastic composites including the ellipsoidal particles [20, 21] and cylindrical fibers [22, 23]. For the analytic description of the interfacial partial debonding, Zhao YH *et al.* [20, 21] suggested micromechanics-based model of two-phase elastoplastic composite with ellipsoidal particles in which the interfacial partial debonding is considered as double debonding. They substituted the partially debonded isotropic inclusions into fictitious undebonded transversely isotropic inclusions. However, the suggested model has some limitations: (1) the assumed partial debonding situations are not considered as an intermediate part of progressive debonding; (2) the double partial debonding cases are thoroughly unusual in real because of

stress concentration around the micro crack tips. Zheng SF *et al*. [22, 23] suggested modified micromechanics-based interfacial partial debonding model of two-phase elastoplastic composite considering cylindrical filler with providing FE solutions. The suggested model can depict on interfacial partial debonding as a single debonding and the amount of partial debonding is determined by debonding angle. Nevertheless, the suggested model still cannot provide proper analytic solution for IPPD of ellipsoidal inclusions. Furthermore, the aforementioned models have not handled the toughening behaviors of the reinforced fillers including the microscopic energy dissipation.

In this study, multiscale FE analysis framework that can consider influences of IPPD on fracture toughness of nanocomposites with spherical nanoparticles is constructed. To the best of our knowledge, there is no study or models in which IPPD is considered to analyze fracture toughness enhancement of nanocomposites in viewpoint of energy dissipation. In result of aforementioned study by Zheng SF *et al*. [22, 23], decrease of the Young's modulus of the two-phase nanocomposites is observed as partial debonding progresses until it reaches to debonding angle threshold. In this light, it is worthy to investigate influences of IPPD on fracture toughness of nanocomposites. With an expectation that the nanoparticles with IPPD have different energy dissipation behaviors from the uniformly debonded nanoparticles, the multiscale analysis with conceptualization of the toughening mechanism as shown in Figure 2 (a) and (b) is conducted to

investigate an influence of the IPPD on the fracture toughness enhancement of polymer nanocomposites. I expect that results from the multiscale analysis can be a proper guideline of applying IPPD in analysis on the toughness enhancement of nanocomposites with parameterization of interfacial fracture energy and volume fraction of particles as well as specific debonding area (SDA) of the micro cracks.

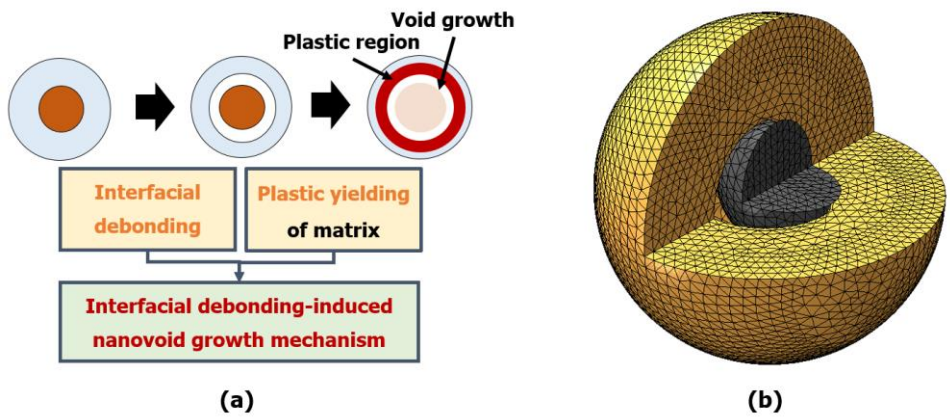

Figure 2. Conceptualization of the interfacial debonding-induced nanovoid growth mechanism: (a) conceptual schema of sub-mechanisms and (b) FE model depicting on the mechanisms.

2. Methodology and models

2.1. Description of the multiscale strategy

A multiscale framework is proposed to quantify the fracture toughness enhancement induced by interfacial debonding-induced nanovoid growth mechanism, which is composed of two sub-mechanisms: interfacial debonding of nanoparticles and following plastic nanovoid growth. A multiscale approach is useful to describe the polymer nanocomposites using the RVE. The fracture toughness enhancement of polymer nanocomposites due to the toughening mechanisms can be obtained from the following form:

$$\Delta G_i = 2 \times \int_0^{\rho^*(\phi=\pi/2)} u_i d\rho \tag{1}$$

where i is an index of each toughening mechanism (i=db; interfacial debonding and i=py; plastic nanovoid growth), ΔG_i is toughness enhancement of each toughening mechanism and u_i is dissipated energy density of each toughening mechanism. Therefore, the computation of dissipated energy density of each toughening mechanism is necessary to obtain the fracture toughness enhancement of polymer nanocomposites. From the micromechanics approach, the link between the macroscopic stress/strain fields and the microscopic stress/strain fields can be quantified as follows:

$$\{\boldsymbol{\Sigma}, \mathbf{E}\} = \frac{1}{|Y|} \int_Y \{\boldsymbol{\sigma}, \boldsymbol{\varepsilon}\} dV_y \tag{2}$$

where $\boldsymbol{\Sigma}$ is macroscopic stress, $\mathbf{E}$ is macroscopic strain, $\boldsymbol{\sigma}$ is microscopic stress, $\boldsymbol{\varepsilon}$ is microscopic strain and Y is the domain of RVE. Using the Mori-Tanaka approach [24], the RVE is simplified to the two-phase model with spherical particle phase and concentric hollow sphere matrix phase. Only hydrostatic macroscopic stress/strain fields are considered by neglecting the shape deformation resulting from the deviatoric macroscopic stress/strain fields. The assumption relies on the existing study [25] that effect of void expansion on the model is much larger than effect of shape deformation when value of mean normal stress is significantly high. I considered a radius of nanoparticle higher than 10nm, and the interface effect that comes from the highly densified polymeric domain (*i.e.*, interphase zone) was neglected [26], thus two-phase nanocomposite models including particle and matrix are considered in this study.

As mentioned in introduction, Zappalorto M *et al*. [17-19] proposed the analytic model of fracture toughness enhancement of polymeric nanocomposites with assumption of uniformly debonded nanoparticles. In the following subsections, after brief review of the analytic model considering uniformly debonded nanoparticles, multiscale framework to predict the fracture toughness of polymer nanocomposites including the IPPD of nanoparticles is proposed with finite element (FE) analysis.

2.2. Review of fracture toughness enhancement due to uniformly debonded nanoparticles

Zappalorto M *et al*. [17-19] proposed the analytical toughness enhancement model of polymeric nanocomposites considering the debonding of interfaces and plastic nanovoid growth as toughening mechanisms. The critical stress, the minimum interfacial stress to cause debonding of interface, can be obtained by Eq. (3) [18, 19, 27-29]:

$$\sigma_{\mathrm{cr}} \cong \sqrt{\frac{4\gamma_{\mathrm{db}}}{r_0}\frac{E_{\mathrm{m}}}{1+\nu_{\mathrm{m}}}} \tag{3}$$

where γ_{db} is an interfacial fracture energy between silica and epoxy, E_{m} is Young's modulus of the matrix, ν_{m} is Poisson's ratio of the matrix and r_0 is radius of the particle. When the critical stress is subjected to the interface, incipient debonding occurs where the hydrostatic critical stress on analytical RVE of nanocomposites is denoted as $\sigma_{\mathrm{cr}}^{\mathrm{h}}$. When interfacial stress reaches to the critical stress, the hydrostatic critical stress can be obtained by Eq. (4) [17-19, 29]:

$$\sigma_{\mathrm{cr}}^{\mathrm{h}} = \overline{\sigma_{\mathrm{cr}}^{\mathrm{h}}} = \frac{1}{\rho^*(\phi=\pi/2)} \times \int_0^{\rho^*(\phi=\pi/2)} \sigma_{\mathrm{cr}}^{\mathrm{h}} d\rho = 2 \times C_{\mathrm{h}} \times \sigma_{\mathrm{cr}} \tag{4}$$

where ρ^* is maximum distance of active process zone from the macroscopic crack tip along the vertical direction, ϕ is an angle from macroscopic crack tip direction and C_{h} is the reciprocal of the hydrostatic

part of the global stress concentration tensor [19, 28, 29] which can be obtained by the following form of zero-interphase:

$$C_{\mathrm{h}} \cong \frac{(3K_{\mathrm{p}}+4G_{\mathrm{m}})}{(3K_{\mathrm{m}}+4G_{\mathrm{m}})}+\frac{4G_{\mathrm{m}}(K_{\mathrm{p}}-K_{\mathrm{m}})}{K_{\mathrm{m}}(3K_{\mathrm{m}}+4G_{\mathrm{m}})}\times\left(\frac{r_0}{\mathrm{b}}\right)^3 \tag{5}$$

where K_{p} is bulk modulus of the particle, K_{m} is bulk modulus of the matrix, G_{m} is shear modulus of the matrix and b is radius of spherical RVE, respectively. Toughness enhancement by each toughening mechanisms then can be obtained by Eq. (25-1) and (25-2) with considering above critical stress and hydrostatic critical stress.

As interfacial uniform debonding of particle is assumed to obtain the energy dissipation by each toughening mechanism in the above model, it cannot represent the IPPD phenomenon.

2.3. Fracture toughness enhancement due to IPPD of nanoparticles

2.3.1. Preparation of finite element models

To quantify the plastic nanovoid growth resulting in plastic yielding of matrix with consideration of IPPD, I construct FE models including partial debonding of nanoparticles. From the Mori-Tanaka approach [24], the RVE of nanocomposites includes only single inhomogeneity (spherical nanoparticle) and hollow-shaped matrix domain with concentricity.

Hereby it is assumed that: (1) all the particles in active process zone underwent the same IPPD sequence by increasing SDA when hydrostatic critical stress is applied on surface of the each particle phase, and (2) all the

particles reached to the final state are in stable, without any singular instable behavior.

The above assumptions obviously cannot be in the real case, but as I are primarily interested in the effects of the toughening mechanisms affected by the IPPD sequence, such an idealization allows it to focus on the effects in a simple fashion. With the above assumptions, the FE model including the single nanoparticle is regarded as the RVE of nanoparticulate composites with partial debonding.

In order to investigate an influence of the IPPD of nanoparticles on the fracture toughness enhancement of polymer nanocomposites, I constructed the seven different types of FE models (Figure 3) of RVE for different SDA that is area of partial debonding divided by area of uniform debonding as the following form:

$$\xi = \frac{A_{\mathrm{db}}}{A_{\mathrm{db}}^{\max}} \tag{6}$$

Specifically, when the SDA is 0, the particle and matrix are in full contact state and if the SDA is 1, the particle and matrix are in uniformly debonded state. It is assumed that there is only single microcrack on the interface between matrix and nanoparticle. For the construction of FE models, commercial software ABAQUS® (Dassault Systems® Inc.) [30] is employed. The elastic properties of the each phase and nanocomposites are listed in Table I. The elastic properties of nanocomposites in Table I are calculated in section 2.3.2 via micromechanics considering Mori-Tanaka approach [24]. It

is assumed that, for simplicity, the stress-strain relationship of the matrix phase beyond the yield point follows hardening behavior of the matrix as a below power law [19, 31]:

$$\frac{\bar{\varepsilon}}{\varepsilon_{\mathrm{Y}}}=\left(\frac{\bar{\sigma}}{\sigma_{\mathrm{Y}}}\right)^{n} \quad \text{if} \quad \bar{\sigma}\geq\sigma_{\mathrm{Y}} \tag{7}$$

where $\bar{\varepsilon}$ is equivalent strain, $\bar{\sigma}$ is equivalent stress, ε_{Y} is yield strain, σ_{Y} is yield stress and n is hardening exponent. The yield stress of the epoxy matrix used in this study is equal to $0.068\,\mathrm{MPa}$, with hardening exponent, 3, for appropriate description of hardening behavior of matrix [17, 19]. It is noted that plasticity of the whole composites is not considerable, as only information about plasticity of matrix is used in obtaining the toughness enhancement of the composites in following sections 2.3.3 and 2.3.4.

To conduct parametric study on the volume fraction of nanoparticles, 42 FE models are constructed for different volume fraction of nanoparticles (1% to 6%) and different SDA (0 to 1). Radii of the FE models of silica and silica/epoxy composite are listed in Table II. Specifically, Model I represents full contact case and Model II-VI represent partial debonding cases, and Model VII represents uniform debonding case when debonding occurs between nanoparticle and matrix.

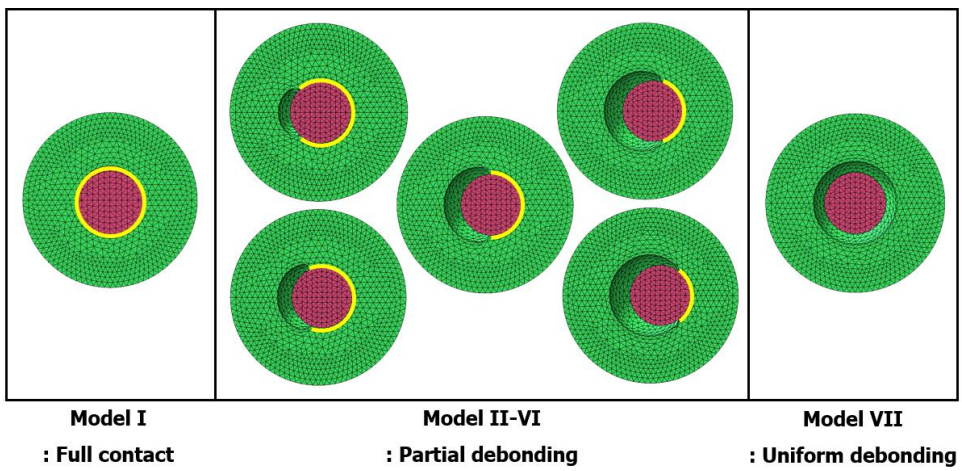

Figure 3. FE models of interfacial partial debonding for different specific debonding area (0, 0.167, 0.333, 0.500, 0.667, 0.833 and 1.000) at a 6% particle volume fraction and experimental interfacial fracture energy of $0.065118\ J/m^2$ with representing partial contact area as yellow curve on each model.

Table I. Elastic properties of silica and epoxy (obtained from MD simulation) [32, 33] and silica/epoxy composite (obtained from micromechanics [34])

Elastic properties	Silica	Epoxy	Silica/epoxy nanocomposites					
			Particle volume fraction, %					
			1	2	3	4	5	6
Young′s modulus, *GPa*	104	3.65	3.73	3.81	3.89	3.97	4.05	4.14
Poisson′s ratio	0.4054	0.37	0.369	0.368	0.368	0.367	0.366	0.365

Table II. Radii of silica and silica/epoxy composite of FE model

	silica	Silica/epoxy nanocomposites					
		Particle volume fraction, %					
		1	2	3	4	5	6
Radius, nm	15	69.6	55.3	48.3	43.9	40.7	38.3

2.3.2. Quantification of elastic properties of nanocomposites via micromechanics

Material properties of silica/epoxy nanocomposites with varying particle volume fraction in Table I can be obtained from multi-inclusion model suggested by Yang S and Cho M [32]. By this model, overall elastic stiffness tensor of the nanocomposites ($\mathbf{C}$) can be expressed to consist of matrix phase (r = 1) with nanoparticle phase (r = 2) and it is expressed by Eq. (8):

$$\mathbf{C} = \mathbf{C}_{\text{inf}} \left[\mathbf{I} + (\mathbf{S} - \mathbf{I}) \left(\sum_{r=1}^{2} f_r \mathbf{\Phi}_r \right) \right]^{-1} \left[\mathbf{I} + \mathbf{S} \left(\sum_{r=1}^{2} f_r \mathbf{\Phi}_r \right) \right]^{-1} \tag{8}$$

where $\mathbf{C}_{\text{inf}}$ is the stiffness tensor of the infinite medium, f_r is the volume fraction of the r$^{\text{th}}$ phase, $\mathbf{S}$ is the Eshelby's tensor and $\mathbf{I}$ is the identity tensor. $\mathbf{\Phi}_r$ is the eigenstrain concentration tensor of the r$^{\text{th}}$ phase and it is expressed in Eq. (9):

$$\mathbf{\Phi}_r = \left[\left(\mathbf{C}_{\text{inf}} - \mathbf{C}_r \right)^{-1} \mathbf{C}_{\text{inf}} - \mathbf{S} \right]^{-1} \tag{9}$$

where $\mathbf{C}_r$ is the stiffness tensor of the r$^{\text{th}}$ phase. The eigenstrain of r$^{\text{th}}$ phase ($\boldsymbol{\varepsilon}_r^*$) can be represented by Eq. (10):

$$\boldsymbol{\varepsilon}_r^* = \mathbf{\Phi}_r \boldsymbol{\varepsilon}^0 \tag{10}$$

where $\boldsymbol{\varepsilon}^0$ is macroscopic strain. It is confirmed that when particle radius is getting bigger than 1.5nm, Young's modulus of silica/epoxy nanocomposites obtained from the MD simulation converges to which obtained from micromechanics model suggested by Mori and Tanaka [24, 26].

2.3.3. Finite element analysis of representative volume element

As mentioned in the previous section, the volume average of microscopic strain fields is same with the macroscopic strain from the micromechanics theory. As the incipient interfacial debonding occurs at the hydrostatic critical macroscopic strain ($\varepsilon_{\mathrm{cr}}^{\mathrm{h}}$), the input of FE homogenization analysis via software ABAQUS® for the macroscopic strain fields are determined by $\varepsilon_{\mathrm{cr}}^{\mathrm{h}}$. The hydrostatic critical macroscopic strain can be calculated as follows [19]:

$$\varepsilon_{\mathrm{cr}}^{\mathrm{h}} = \varepsilon_{\mathrm{rr}}^{\mathrm{el}}\Big|_{r=r_{\mathrm{m}}} = \frac{\sigma_{\mathrm{cr}}^{\mathrm{h}}}{3K_{\mathrm{comp}}} \quad (R_{\mathrm{P}} < r_0) \tag{11}$$

where $\varepsilon_{\mathrm{rr}}^{\mathrm{el}}$ is radial component of elastic strain of nanocomposites, K_{comp} is the bulk modulus of nanocomposites, r_0 is radius of particle and

$$\varepsilon_{\mathrm{cr}}^{\mathrm{h}} = \varepsilon_{\mathrm{rr}}^{\mathrm{el}}\Big|_{r=r_{\mathrm{m}}} = \frac{\sigma_{\mathrm{cr}}^{\mathrm{h}}}{3K_{\mathrm{m}}} - \frac{2\sigma_{\mathrm{Ym}}R_{\mathrm{P}}^{3}(1+\nu_{\mathrm{m}})}{3E_{\mathrm{m}}r_{\mathrm{m}}^{3}} \quad (R_{\mathrm{P}} > r_0) \tag{12}$$

where K_{m} is the bulk modulus of matrix, σ_{Ym} is yield stress of matrix, ν_{m} is Poisson's ratio of matrix, E_{m} is Young's modulus of matrix, r_{m} is the external radius of RVE, and R_{p} is the radius of plastic region on matrix, which can be obtained by the following equation [19]:

$$R_{\mathrm{P}} = r_0 \times \left\{ \frac{3\sigma_{\mathrm{cr}}^{\mathrm{h}}}{2\sigma_{\mathrm{Ym}}n_{\mathrm{m}}} - \left(\frac{1}{n_{\mathrm{m}}} - 1 \right) \right\}^{\frac{n_{\mathrm{m}}}{3}} \tag{13}$$

where and n_{m} is hardening exponent of the matrix. The detail procedure of

FE homogenization analysis to quantify the dissipated plastic deformation energy of RVE is summarized in the Appendix.

2.3.4. Quantification of fracture toughness enhancements

A schematic representation of the proposed multiscale framework is presented in Figure 4. The dissipated energy includes the interfacial debonding energy and plastic deformation energy by following plastic nanovoid growth. Using the dissipated plastic energy obtained from the FE models, the fracture toughness enhancement of nanocomposites induced by the partial debonding of interfaces is quantified using the proposed multiscale method. Detailed description of the multiscale model is explained in the following subsections.

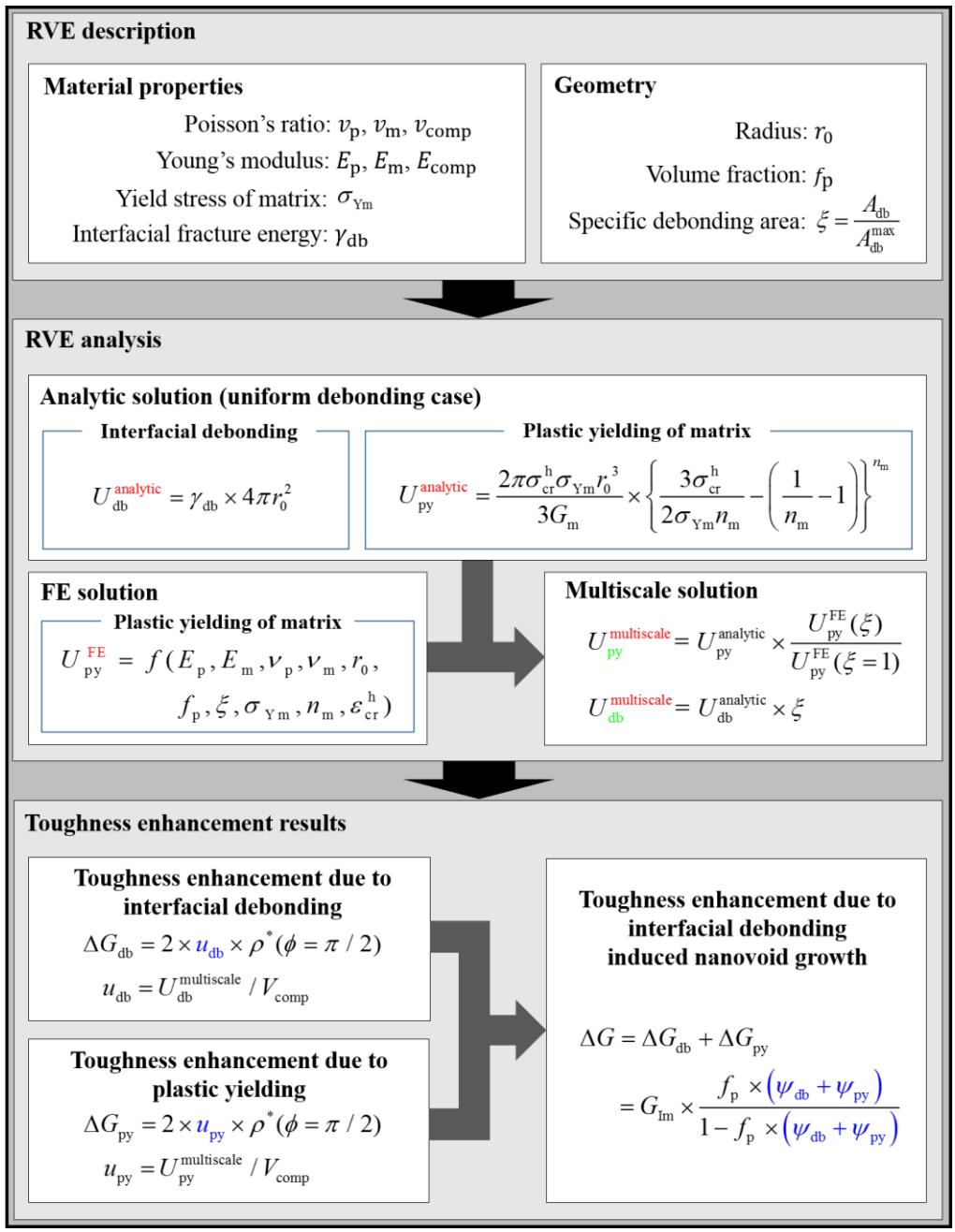

Figure 4. A schematic representation of the proposed multiscale framework

2.3.4.1. Interfacial debonding-induced fracture toughness enhancement

The dissipated energy from the interfacial debonding of nanoparticles ($U_{\mathrm{db}}^{\mathrm{analytic}}$) can be quantified as the following form [18, 19, 27]:

$$U_{\mathrm{db}}^{\mathrm{analytic}} = \gamma_{\mathrm{db}} \times 4\pi r_0^2 \tag{14}$$

Then the dissipated energy from the interfacial partial debonding of nanoparticles can be obtained as the following form:

$$U_{\mathrm{db}}^{\mathrm{multiscale}} = \gamma_{\mathrm{db}} \times 4\pi r_0^2 \times \xi \tag{15}$$

in which effect of partial debonding is considered by applying SDA. The above Eq. (15) can be expressed into following energy density form:

$$u_{\mathrm{db}} = U_{\mathrm{db}}^{\mathrm{multiscale}} / V_{\mathrm{comp}} \tag{16}$$

where V_{comp} is volume of each RVE model of the nanocomposites.

Therefore, the fracture toughness enhancement due to interfacial debonding (ΔG_{db}) can be computed as follows:

$$\Delta G_{\mathrm{db}} = 2 \times \int_0^{\rho^*(\phi=\pi/2)} u_{\mathrm{db}} d\rho = f_{\mathrm{p}} \times \psi_{\mathrm{db}} \times G_{\mathrm{Ic}} \tag{17}$$

where ψ_{db} is the contribution of the interfacial debonding mechanism per unit volume fraction of nanoparticles, which can be computed as follows [18, 19, 28]:

$$\psi_{\mathrm{db}} = \frac{2}{3\pi} \times \frac{\gamma_{\mathrm{db}}}{r_0} \times \frac{1+\nu_{\mathrm{comp}}}{1-\nu_{\mathrm{comp}}} \times \frac{E_{\mathrm{comp}}}{\sigma_{\mathrm{cr}}^2 (C_{\mathrm{h}})^2} \times \xi \tag{18}$$

where ν_{comp} is Poisson's ratio of the nanocomposites and E_{comp} is Young's modulus of the nanocomposites, respectively.

2.3.4.2. Plastic yielding of nanovoids-induced fracture toughness enhancement

The dissipated energy of plastic yielding of matrix due to the nanovoid growth around nanoparticle under uniform debonding ($U_{\mathrm{py}}^{\mathrm{analytic}}$) can be computed by the analytic form [19]:

$$U_{\mathrm{py}}^{\mathrm{analytic}} = \frac{2\pi\sigma_{\mathrm{cr}}^{\mathrm{h}}\sigma_{\mathrm{Ym}}r_0^3}{3G_{\mathrm{m}}} \times \left\{ \frac{3\sigma_{\mathrm{cr}}^{\mathrm{h}}}{2\sigma_{\mathrm{Ym}}n_{\mathrm{m}}} - \left(\frac{1}{n_{\mathrm{m}}} - 1 \right) \right\}^{n_{\mathrm{m}}} \tag{19}$$

where G_{m} is shear modulus of the matrix. Then, the dissipated energy of plastic yielding of matrix due to the nanovoid growth around nanoparticle with partial debonding ($U_{\mathrm{py}}^{\mathrm{multiscale}}$) can be described as following combination form:

$$U_{\mathrm{py}}^{\mathrm{multiscale}}(\xi) \equiv U_{\mathrm{py}}^{\mathrm{analytic}} \times \varsigma(\xi) \tag{20}$$

where $U_{\mathrm{py}}^{\mathrm{multiscale}}$ is the dissipated energy of plastic yielding of matrix obtained from the multiscale analysis and the ratio, ς, is defined as follows:

$$\varsigma(\xi) = \frac{U_{\mathrm{py}}^{\mathrm{FE}}(\xi)}{U_{\mathrm{py}}^{\mathrm{FE}}(\xi = 1)} \tag{21}$$

where $U_{\mathrm{py}}^{\mathrm{FE}}$ is the dissipated energy of plastic yielding of matrix obtained from the FE analysis via software ABAQUS®. The values of $U_{\mathrm{py}}^{\mathrm{FE}}$ are used only to represent overall tendency on change of the dissipated plastic energy for different cases of partial debonding rather than the magnitudes of the

dissipated plastic energy because of difficulties on order matching. Methodology for using the dissipated plastic energy itself on the multiscale analysis model will be studied in the future work. The values of $U_{\mathrm{py}}^{\mathrm{analytic}}$ represent analytic result of the dissipated plastic energy for the case of uniform debonding, thus $U_{\mathrm{py}}^{\mathrm{multiscale}}$ can be regarded as representation of the dissipated energy of plastic yielding of matrix with combination of the $U_{\mathrm{py}}^{\mathrm{analytic}}$ and $U_{\mathrm{py}}^{\mathrm{FE}}$. The previously mentioned dissipated energy of plastic yielding of matrix in Eq. (20) can be expressed into below energy density form:

$$u_{\mathrm{py}} = U_{\mathrm{py}}^{\mathrm{multiscale}} / V_{\mathrm{comp}} \tag{22}$$

As a result, the fracture toughness enhancement (ΔG_{py}) induced by the plastic nanovoid growth mechanism can be obtained as the following form:

$$\Delta G_{\mathrm{py}} = 2 \times \int_0^{\rho^*(\phi=\pi/2)} u_{\mathrm{py}} d\rho = f_{\mathrm{p}} \times \psi_{\mathrm{py}} \times G_{\mathrm{Ic}} \tag{23}$$

where ψ_{py} is the contribution of the plastic nanovoid growth mechanism per unit volume fraction of nanoparticles, which can be organized as following form [19, 28]:

$$\psi_{\mathrm{py}} = \frac{2}{9\pi C_{\mathrm{h}}} \times \frac{1+\nu_{\mathrm{comp}}}{1-\nu_{\mathrm{comp}}} \times \frac{E_{\mathrm{comp}}}{G_{\mathrm{m}}} \times \frac{\sigma_{\mathrm{Ym}}}{\sigma_{\mathrm{cr}}} \times \left\{ 3C_{\mathrm{h}} \times \frac{\sigma_{\mathrm{cr}}}{\sigma_{\mathrm{Ym}} n_{\mathrm{m}}} - \left(\frac{1}{n_{\mathrm{m}}} - 1 \right) \right\}^{n_{\mathrm{m}}} \times \varsigma \tag{24}$$

Finally, toughness enhancement of the nanocomposites by interfacial debonding-induced nanovoid growth with consideration of interfacial partial debonding is obtained by summation of the toughness enhancement of each

toughening mechanism, as following form:

$$\Delta G_{\mathrm{db}} + \Delta G_{\mathrm{py}} = 2 \times \int_0^{\rho^*(\phi=\pi/2)} \left(u_{\mathrm{db}} + u_{\mathrm{py}} \right) d\rho = 2 \times \left(u_{\mathrm{db}} + u_{\mathrm{py}} \right) \times \rho^* (\phi = \pi / 2) \quad (25\text{-}1)$$

The Eq. (25-1) can be rearranged into a form consisting of fracture toughness of pure matrix (G_{Im}) and terms of the contribution of each toughening mechanism as below:

$$\Delta G_{\mathrm{db}} + \Delta G_{\mathrm{py}} = G_{\mathrm{Im}} \times \frac{f_{\mathrm{p}} \times \left(\psi_{\mathrm{db}} + \psi_{\mathrm{py}} \right)}{1 - f_{\mathrm{p}} \times \left(\psi_{\mathrm{db}} + \psi_{\mathrm{py}} \right)} \quad (25\text{-}2)$$

The toughness enhancement of the composites with interfacial debonding-induced nanovoid growth mechanism by Eq. (25-2) can be directly obtained as the fracture toughness of the pure matrix is known.

3. Results and discussion

I investigated an influence of SDA on the fracture toughness enhancement of epoxy nanocomposites with the purpose of providing insight of applying the progressive-partial debonding phenomenon in analysis on the toughness enhancement of nanocomposites by multiscale analysis model. The analysis is conducted for four different interfacial fracture energy systems of 0.065118, 0.07, 0.08 and 0.1 J/m^2 with increasing particle volume fraction of 1, 2, 3, 4, 5 and 6 % and with varying SDA of 0, 0.167, 0.333, 0.5, 0.667, 0.833 and 1. It is noted that, as there exists no exact value of interfacial fracture energy of the silica/epoxy nanocomposites with silica radius in Table II, proper value (0.065118 J/m^2) is obtained by conducting least-squares method on values of interfacial fracture energy of existing studies [9, 35]. The other values of increased interfacial fracture energy presented above are parameterized to investigate the cases in which debonding processes become harder. Experimental value of 283.2 J/m^2 [12] is used as a fracture toughness of pure matrix for Eq. (25-2) in this study and the value is expressed as an initial fracture toughness of the each graph in Figure 5.

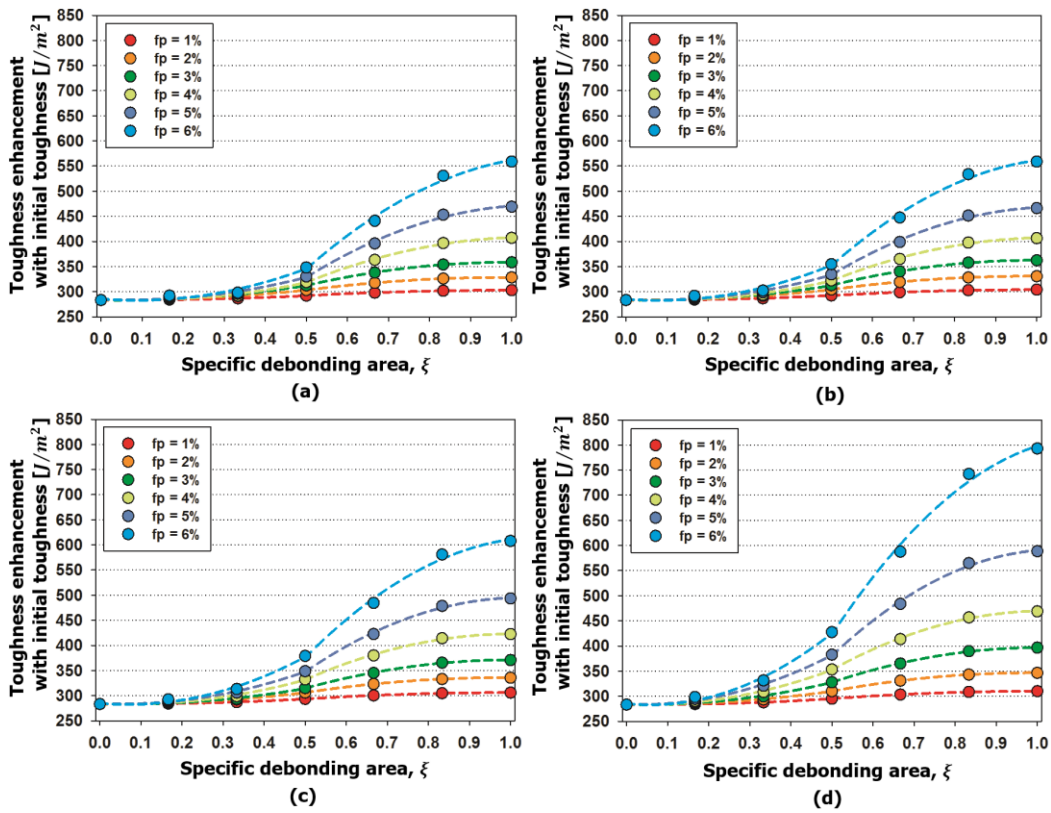

Figure 5. Toughness enhancement of the multiscale model with initial fracture toughness by specific debonding area for different interfacial fracture energy: (a) 0.065118, (b) 0.07, (c) 0.08 and (d) 0.1 J / m^2.

Results of the simulation in Figure 5 show that values of the fracture toughness enhancement monotonically increase when SDA increases from 0 to 1. For every increasing SDA, higher toughness enhancement is observed when volume fraction of the particle is high. It can be confirmed that toughness enhancement value for each particle volume fraction and SDA case becomes higher as the interfacial fracture energy increases from 0.065118 to $0.1\,J/m^2$ as shown in Figure 5 (a), (b), (c) and (d). For toughness enhancement, increase of particle volume fraction means that the nanocomposite have more opportunities of undergoing interfacial debonding-induced nanovoid growth mechanism. Meanwhile, the increase of interfacial fracture energy compels the interfacial debonding process of nanocomposite to become harder. As a result, more internal energy of the nanocomposite is required to go through the interfacial debonding process. It can be also observed that the toughness enhancement rapidly increase after midpoint of SDA for each interfacial fracture energy and particle volume fraction case. As the dissipated energy from the interfacial partial debonding mechanism is linearly proportional to the SDA, the rapid increase of the toughness enhancement refers to boost of energy dissipation due to plastic yielding of matrix mechanism.

The aforementioned discussions can only be conducted by the multiscale analysis model, since the existing analysis models cannot handle the IPPD sequence in viewpoint of microscopic energy dissipations with SDA concept which needs the FE simulation approach used in this paper.

4. Conclusions

In this study, an influence of progressive-partial debonding on the toughness enhancement of silica/epoxy nanocomposites is investigated. The simulation results show that the fracture toughness enhancement due to the progressive-partial debonding of nanoparticles is influenced by factors such as particle volume fraction, SDA and interfacial fracture energy. The suggested multiscale analysis methodology is expected to contribute the material design of high toughness materials with large amount of plastic energy dissipation by providing analysis on progressive-partial debonding sequence with the energy dissipation mechanisms. For instance, it will be very helpful to investigate experimental results of toughness enhancement. In real case, as shown in Figure 1, there exist many partially debonded fillers in nanocomposites even after experimental sequence is finished. Though the existing analysis models have difficulty in predicting precise fracture toughness results, the suggested mulstiscale analysis model enables to predict more reliable value of effective toughness enhancement of the nanocomposite by considering toughening mechanisms on progressive-partial debonding sequence with investigation of the amount of partially debonded fillers with representative SEM images. Applying the multiscale analysis model, material design of polymer nanocomposites can be achieved by using the local grafting of CNT [36] or control of local defects of

graphene [37] and CNT [38, 39]. It is expected that the multiscale methodology suggested by this study can provide insight for handling partial debonding phenomenon into toughness analysis of the nanocomposites, especially as an analytical tool for optimal design of the nanocomposites materials, quantification of influence of partial debonding on the each toughening mechanism and evaluation of the performance of the nanocomposites. In future works, these works will be extended to the ellipsoidal nanoparticles and three-phase nanocomposites models including interphase zone.

Appendix

In multiscale homogenization scheme, the microscopic stress fields can be described by the following form:

$$\boldsymbol{\sigma} = \boldsymbol{\sigma}\left(\nabla_{\mathbf{x}}\mathbf{u}_0 + \nabla_{\mathbf{y}}\mathbf{u}_1\right) \tag{A1}$$

where $\mathbf{u}_0$ and $\mathbf{u}_1$ are macroscopic and microscopic displacement fields. Using the analogy to the thermomechanical problem (A2), microscopic stress fields and microscopic deformation fields can be obtained by the thermomechanical problem as shown in the following rules (A3):

$$\boldsymbol{\sigma} = \boldsymbol{\sigma}\left(-\boldsymbol{\alpha}\Delta T + \nabla\mathbf{u}\right) \tag{A2}$$

$$\left(\nabla_{\mathbf{x}}\mathbf{u}_0, \nabla_{\mathbf{y}}\mathbf{u}_1\right) \text{ in homogenization } \leftrightarrow \left(-\boldsymbol{\alpha}\Delta T, \nabla\mathbf{u}\right) \text{ in thermomechanics} \tag{A3}$$

Here, $\boldsymbol{\alpha}$ and ΔT are thermal expansion coefficients tensor and the change in temperature, respectively. Using the commercial FE software ABAQUS®, the microscopic stress fields and deformation fields in the multiscale homogenization problem are numerically obtained via the analogy to the thermomechanical problem. The fixed displacement boundary conditions are imposed on the outer surface of RVE. It is determined that the macroscopic strain fields by using the Eq. (12), which is uniform in the RVE. Here, the uniform thermal strain is imposed in the RVE using the aforementioned rule of Eq. (A3). The microscopic deformation and stress fields, and the microscopic plastic energy dissipation are quantified by the post-processing after solving the FE problems in the ABAQUS®.

References

1. Mimura K, Ito H, Fujioka H. Improvement of thermal and mechanical properties by control of morphologies in PES-modified epoxy resins. Polymer 2000; 41: 4451-9.
2. Yu S, Yang S, Cho M. Multi-scale modeling of cross-linked epoxy nanocomposites. Polymer 2009; 50: 945-52.
3. Yang S, Yu S, Cho M. Sequential thermoelastic multiscale analysis of nanoparticulate composites. J Appl Phys 2010; 108: 056102.
4. Johnsen BB, Kinloch AJ, Mohammed RD, Taylor AC, Sprenger S. Toughening mechanisms of nanoparticle-modified epoxy polymers. Polymer 2007; 48: 530-41.
5. Ma J, Mo MS, Du XS, Rosso P, Friedrich K, Kuan HC. Effect of inorganic nanoparticles on mechanical property, fracture toughness and toughening mechanism of two epoxy systems. Polymer 2008; 49: 3510-23.
6. Liang YL, Pearson RA. Toughening mechanisms in epoxy-silica nanocomposites (ESNs). Polymer 2009; 50: 4895-905.
7. Hsieh TH, Kinloch AJ, Masania K, Lee JS, Taylor AC, Sprenger S. The toughness of epoxy polymers and fibre composites modified with rubber microparticles and silica nanoparticles. J Mater Sci 2010; 45: 1193-210.
8. Hsieh TH, Kinloch AJ, Masania K, Taylor AC, Sprenger S. The mechanisms and mechanics of the toughening of epoxy polymers

modified with silica nanoparticles. Polymer 2010; 51: 6284-94.

9. Williams JG. Particle toughening of polymers by plastic void growth. Compos Sci Technol 2010; 70: 885-91.
10. Dittanet P, Pearson RA. Effect of silica nanoparticle size on toughening mechanisms of filled epoxy. Polymer 2012; 53: 1890-905.
11. Bray DJ, Dittanet P, Guild FJ, Kinloch AJ, Masania K, Pearson RA, Taylor AC. The modelling of the toughening of epoxy polymers via silica nanoparticles: The effects of volume fraction and particle size. Polymer 2013; 27: 2763-9.
12. Zamanian M, Mortezaei M, Salehnia B, Jam JE. Fracture toughness of epoxy polymer modified with nanosilica particles: Particle size effect. Eng Fract Mech 2013; 97: 193-206.
13. Yu F, Huang HX. Simultaneously toughening and reinforcing poly(lactic acid)/thermoplastic polyurethane blend via enhancing interfacial adhesion by hydrophobic silica nanoparticles. Polym Test 2015; 45: 107-13.
14. Liu S, Fan X, He C. Improving the fracture toughness of epoxy with nanosilica-rubber core-shell nanoparticles. Compos Sci Technol 2016; 125: 132-40.
15. Kinloch AJ, Shaw AJ, Tod DA, Hunston DL. Deformation and fracture behavior of a rubber-toughened epoxy: 1. Microstructure and fracture studies. Polymer 1983; 24: 1341-54.
16. Kawaguchi T, Pearson RA. The effect of particle-matrix adhesion on the

mechanical behavior of glass filled epoxies. Part 2. A study on fracture toughness. Polymer 2003; 44: 4239-47.

17. Zappalorto M, Salviato M, Quaresimin M. Assessment of debonding-induced toughening in nanocomposites. Precedia Eng 2011; 10: 2973-8.

18. Salviato M, Zappalorto M, Quaresimin M. Plastic yielding around nanovoids. Procedia Eng 2011; 10: 3316-21.

19. Zappalorto M, Salviato M, Quaresimin M. A multiscale model to describe nanocomposite fracture toughness enhancement by the plastic yield of nanovoids. Compos Sci Technol 2012; 72: 1683-91.

20. Zhao YH, Weng GJ. Plasticity of a two-phase composite with partially debonded inclusions. Int J Plasticity 1996; 12: 781-804.

21. Zhao YH, Weng GJ. Transversely isotropic moduli of two partially debonded composites. Int J Solids Struct 1997; 34: 493-507.

22. Zheng SF, Denda M, Weng GJ. Interfacial partial debonding and its influence on the elasticity of a two-phase composite. Mech Mater 2000; 32: 695-709.

23. Zheng SF, Denda M, Weng GJ. Overall elastic and elastoplastic behavior of a partially debonded fiber-reinforced composite. J Compos Mater 2003; 37: 741-58.

24. Mori T, Tanaka K. Average stress in matrix and average elastic energy of materials with misfitting inclusions. Acta Metall Mater 1973; 21: 571-4.

25. Rice JR, Tracy DM. On ductile enlargement of voids in triaxial stress fields. J Mech Phys Solids 1969; 17: 210-7.

26. Yang S, Cho M. Scale bridging method to characterize mechanical properties of nanoparticle/polymer nanocomposites. Appl Phys Lett 2008; 93: 043111.

27. Chen JK, Huang ZP, Zhu J. Size effect of particles on the damage dissipation in nanocomposites. Compos Sci Technol 2007; 67: 2990-6.

28. Quaresimin M, Salviato M, Zappalorto M. A multi-scale and multi-mechanism approach for the fracture toughness assessment of polymer nanocomposites. Compos Sci Technol 2014; 91: 16-21.

29. Zappalorto M, Salviato M, Quaresimin M. Influence of the interphase zone on the nanoparticle debonding stress. Compos Sci Technol 2011; 72: 49-55.

30. ABAQUS/CAE Version 6.12; 2012.

31. Lazzarin P, Zappalorto M. Plastic notch stress intensity factors for pointed V-notches under antiplane shear loading. Int J Fracture 2008; 152: 1-25.

32. Yang S, Cho M. A scale-bridging method for nanoparticulate polymer nanocomposites and their nondilute concentration effect. Appl Phys Lett 2009; 94: 223104.

33. Choi J, Shin H, Yang S, Cho M. The influence of nanoparticle size on the mechanical properties of polymer nanocomposites and the associated interphase region: A multiscale approach. Compos Struct 2015; 119: 365-376.

34. Shin H, Chang S, Yang S, Youn BD, Cho M. Statistical multiscale

homogenization approach for analyzing polymer nanocomposites that include model inherent uncertainties of molecular dynamics simulations. Compos Part B-Eng 2016; 87: 120-31.

35. Nakamura Y, Yamaguchi M, Kitayama A, Okubo M, Matsumoto T. Effect of particle size on fracture toughness of epoxy resin filled with angular-shaped silica. Polymer 1991; 32:2221-9.

36. Islam MS, Deng Y, Tong L, Faisal SN, Roy AK, Minett AI, Gomes VG. Grafting carbon nanotubes directly onto carbon fibers for superior mechanical stability: Towards next generation aerospace composites and energy storage applications. Carbon 2016; 96: 701-10.

37. Safaei M, Sheidaei A, Baniassadi M, Ahzi S, Mashhadi MM, Pourboghrat F. An interfacial debonding-induced damage model for graphite nanoplatelet polymer composites. Comp Mater Sci 2015; 96: 191-9.

38. Yang S, Yu S, Cho M. Influence of thrower-stone-wales defects on the interfacial properties of carbon nanotube/polypropylene composites by a molecular dynamics approach. Carbon 2013; 55: 133-43.

39. Yang S, Choi J, Cho M. Intrinsic defect-induced tailoring of interfacial shear strength in CNT/polymer nanocomposites. Compos Struct 2015; 127: 108-19.

Abstract in Korean

본 연구에서는 에폭시-실리카 나노복합재에서 계면 진전 부분 분리가 일어날 때의 인성 향상을 관찰하기 위한 멀티스케일 해석을 수행하였다. 문헌에 의하면, 계면 분리에 따른 나노 공동의 성장은 주요한 인성 향상 메커니즘 중 하나이며, 이는 다시 나노 입자의 계면 분리 메커니즘과 그에 따른 기지의 소성 변형 메커니즘으로 나뉜다. 두 인성 향상 메커니즘에 대하여 계면의 진전 부분 분리를 고려하기 위한 부분 분리 면적을 정의하고, 나노복합재의 미시 응력장에 따른 인성 향상 메커니즘을 관찰하기 위하여 유한요소 해석 모델을 제작하였으며 이들을 적용한 멀티스케일 해석 방법론을 구축하였다. 이러한 방법론을 통해 나노 입자의 계면 진전 부분 분리 메커니즘에 인성 향상을 전체 분리 과정에 대하여 관찰하였으며, 이를 통해 에폭시-실리카 나노복합재의 인성 향상이 계면 파괴 에너지, 부분 분리 면적 및 입자 체적분율이 각각 증가할수록 더 큰 값을 가지게 됨을 확인하였다. 이러한 멀티스케일 해석 모델을 통하여 계면 진전 부분 분리에 따른 나노복합재의 인성 향상에 대해서 보다 엄밀한 해석적 접근을 제공함으로써 관련 연구 분야에 의미있는 통찰을 제시할 수 있을 것으로 기대된다.

Keywords : 나노복합재, 에너지 소산, 인성 향상 메커니즘, 계면 진전 부분 분리, 멀티스케일 해석

Student Number : 2014-22475